NJC

New Journal of Chemistry

A journal for new directions in chemistry

Accepted Manuscript

This article can be cited before page numbers have been issued, to do this please use: T. Xu, J. Huang, M. Fang, W. Zhu, Y. Shentu, M. Sui, C. Li and Y. Zhu, *New J. Chem.*, 2020, DOI: 10.1039/D0NJ04416D.

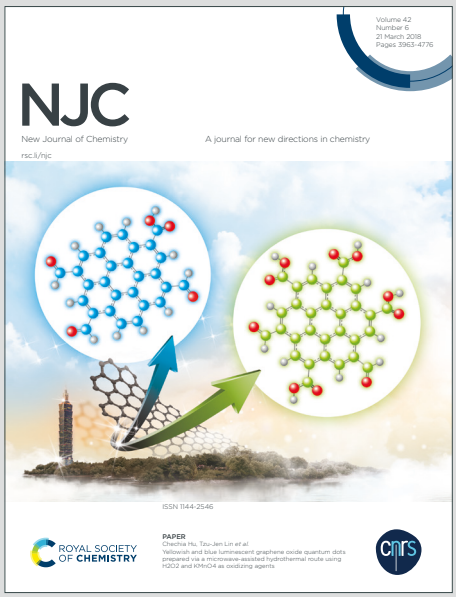

This is an Accepted Manuscript, which has been through the Royal Society of Chemistry peer review process and has been accepted for publication.

Accepted Manuscripts are published online shortly after acceptance, before technical editing, formatting and proof reading. Using this free service, authors can make their results available to the community, in citable form, before we publish the edited article. We will replace this Accepted Manuscript with the edited and formatted Advance Article as soon as it is available.

You can find more information about Accepted Manuscripts in the Information for Authors.

Please note that technical editing may introduce minor changes to the text and/or graphics, which may alter content. The journal's standard Terms & Conditions and the Ethical guidelines still apply. In no event shall the Royal Society of Chemistry be held responsible for any errors or omissions in this Accepted Manuscript or any consequences arising from the use of any information it contains.

NJC A novel "turn-on" fluorescent probe based on naphthalimide for the tracking of lysosomal Cu2+ in living cells

View Article Online
DOI: 10.1039/D0NJ04416D

ARTICLE

A novel "turn-on" fluorescent probe based on naphthalimide for the tracking of lysosomal Cu^{2+} in living cells

Received 00th January 20xx,
Accepted 00th January 20xx

DOI: 10.1039/x0xx00000x

Tingting Xu[a], Junjie Huang[a], Min Fang[a, b]*, Mingshuai Sui[a], Yujing Zhu[a], Yupeng Shentu[a], Cun Li[a, b], Weiju Zhu[a, 3]*

A novel fluorescent probe **CuNI** was synthesized and exhibited highly effect ive fluorescence detection ability for Cu^{2+} in aqueous solution (HOAc-NaOAc buffer, 10 mM, pH 5.0). **CuNI** was obtained with the simple condensation re action between the aldehyde (**MFNI**, bearing naphthalimide fluorescence gr oup**)** and the 2-picolinyl hydrazide which as the Cu^{2+} recognized group. Unde r acidic conditions, **CuNI** showed turn-on fluorescent recognition of Cu^{2+} whi ch could be readily distinguished by the naked eye under 365nm UV lamp an d the detection limit is as low as 19.40 nM. It has been further demonstrate d that **CuNI** was hydrolyzed under the action of Cu^{2+} and the significant incre ase of fluorescence is due to the obvious AIE effect of the hydrolysate **MFNI**. The application of the probe **CuNI** in imaging lysosomal Cu^{2+} in HepG2 cells h as also been demonstrated.

1. Introduction

Copper ion is the third-largest metal trace element in the human body, playing an important role in cell homeostasis [1-4]. The destruction of copper ion homeostasis will cause many diseases. For example, Copper deficiency in the body will induce the diseases of brain-dysfunction, anemia and leukemia [5-7]. And the excessive accumulation of copper ions also leads to a variety of diseases, such as Alzheimer's disease, Menkes disease, Wilson's disease, coronary heart disease and Parkinson's disease [8-11]. The cellular homeostasis of copper is controlled with the copper transporter proteins, such as (human CTR2), which localized in late endosomes and lysosomes [12, 13]. Therefore, it is necessary to study whether the content of Cu^{2+} in lysosomes of human cells is unstable.

Common methods to analyze ion concentration include atomic absorption spectrometry (AAS) [14], inductively coupled plasma mass spectrometry (ICP-MS) [15], voltammetry [16] and others. Because of the complex sample preparation process, these methods need expensive instruments and not suitable for physiological environment. The fluorescent sensors in modern analytical methods have the advantages of high sensitivity, good selectivity, easy sample pretreatment and fast response, which can overcome the shortcomings of traditional methods [17-22]. Before that, many fluorescent probes for detection of coordination binding [23,24] and chemical reactions [25, 26] have been developed. Among them, chemically reactive probes have attracted great attention due to

[a] School of Chemistry and Chemical Engineering, Anhui University, Hefei 230601, PR China
[b] Anhui Province Key Laboratory of Environment-friendly Polymer Materials, Anhui University, Hefei 230601, PR China
[c] Anhui Province Key Laboratory of Chemistry for Inorganic/Organic Hybrid Functionalized Materials, Anhui University, Hefei 230601, PR China

View Article Online
DOI: 10.1039/D0NJ04416D

their high selectivity. Cu^{2+} can generate "fluorescent" products through specific reactions with fluorescent probes to achieve highly selective detection and "turn on" fluorescence response. To date, a few selective fluorescent probes for Cu^{2+} have been investigated utilizing Cu^{2+}-promoted reaction [27-32]. Although there are many reaction-based Cu^{2+} probes using various kinds of fluorophore platforms including rhodamine, coumarin, pyrene, naphthalene, naphthalimide, benzothiazole, the detection systems of these probes need organic solvent as a co-solvent and the detection in complete aqueous solution are still very rare to date. Furthermore, these conventional fluorophores have poor solubility and often possess aggregation-caused quenching (ACQ) phenomenon in pure aqueous solution. In 2001, Tang and his colleagues reported the aggregation-induced emissions (AIE) phenomenon, which can be used to detect analyte in aqueous media and provide good practical use in biological system [33-35]. For now, the fluorescent sensor to recognize lysosomal Cu^{2+} through chemical reaction and AIE phenomenon has rarely reported.

In this work, a novel "turn-on" probe for lysosomal Cu^{2+} was designed and synthesized, which mainly included three portions: (1) a morpholine group as lysosome-target group [36, 37]; (2) 1,8-naphthalimide as chromophore; (3) 2-picolinyl hydrazide group as Cu^{2+} recognized group. It has been proved that **CuNI** has high selectivity to Cu^{2+} not only in aqueous solution but also in cells. Cu^{2+} induced the hydrolysis of **CuNI** in aqueous solution and the product (**MFNI**) lead to the formation of "turn-on" blue fluorescence which caused by the AIE of **MFNI**. Besides, the application of **CuNI** in bioimaging was examined by confocal fluorescence microscopy and it can monitor the lysosomal Cu^{2+} in living HepG2 cells.

2. Experimental

2.1. Materials and instruments

Unless otherwise specified, all commercial grade chemicals and solvents were used without further purification. 4-bromo-1,8-naphthalic anhydride was from Aldrich. N-aminopropylmorpholine, 4-formylphenylboronic acid and 2-picolinyl hydrazide were purchased from Alading Chemical Reagent Co., Ltd (Shanghai, China). The silica gels were obtained from Qingdao Ocean Chemicals (Qingdao, China). Thin layer chromatography (TLC) was carried out using silica gel F254, and column chromatography was conducted over 200 mesh silica gel. The pure water (18.2 MΩ.cm) was obtained with a Milli-Q purification system.

^{1}H NMR spectra were obtained on an AV-600 spectrometer (Bruker, Switzerland) with tetramethylsilane as internal reference.^{13}C NMR spectra were recorded on 151MHz spectrometers. The mass spectra were obtained on a LTQ-Orbitrap XL mass spectrometer. UV-visible absorption spectra were recorded on a UV-1800 spectrophotometer (Shimadzu, Japan). Fluorescence emission spectra were carried out on a LS-55 FL spectrophotometer (PerkinElmer, USA). The fluorescence quantum yields were detected by HORIBA FluoroMax-4P (HORIBA Jobin Yvon) and the results were automatically calculated by the software of the device.

2.2. Synthesis

*2.2.1. N-(morpholinopropyl)- 4-bromo-1,8-naphthalimide **1***

In briefly, 4-bromo-1,8-naphthalic anhydride (2.77 g, 10 mmol) and N-aminopropylmorpholine (2.16 g, 15 mmol) were added to the solution in ethanol (40 mL). The mixture was refluxed at 60 °C for 6 hours. After cooling to room temperature, the precipitate was collected, washed with ethanol for three times, and then dried under vacuum to get a yellow powder 3.49 g (87%). ^{1}H NMR (600 MHz, d6-DMSO) δ 8.58 (dd, J = 12.6, 7.8 Hz, 2H), 8.36 (d, J = 7.8 Hz, 1H), 8.24 (d, J = 7.8 Hz, 1H), 8.04 – 8.00 (m, 1H), 4.13 – 4.10 (m, 2H), 3.38 (d, J = 1.1 Hz, 4H), 2.39 (t, J = 6.7 Hz, 2H), 2.29 (s, 4H), 1.84 – 1.78 (m, 2H). ^{13}C NMR (151 MHz, DMSO) δ 163.53, 163.48, 133.09, 132.05, 131.89, 131.44, 130.34, 129.51, 129.36, 128.91, 123.47, 122.70, 66.53, 56.44, 53.63, 38.98, 24.26. TOF Mass: m/z calcd for $C_{19}H_{19}BrN_2O_3$ ($[M+H]^+$): 403.0652; found 403.0644.

*2.2.2. Synthesis of compound N-(morpholinopropyl)- 4-formylphenyl-1,8-naphthalimide **MFNI***

N-(morpholinopropyl)-4-bromo-1,8-naphthalimide (2.0 g, 5 mmol) and 4-formylphenylboronic acid (1.25 g, 7.5 mmol) were dissolved in a mixture of toluene and ethanol (80 mL, toluene: ethanol = 3:1, v/v), Saturated K_2CO_3 solution (3 mL), and $Pd(PPh_3)_4$ (45 mg) was added. Reflux the reaction mixture under nitrogen for 48 hours. After cooling down to room temperature, the reaction mixture was poured into water and extracted with dichloromethane (3×50 mL). Combined with organic solution, dried by anhydrous magnesium sulfate and concentrated in vacuum. The crude product was purified with a silica gel column using ethyl acetate/petroleum

View Article Online
DOI: 10.1039/D0NJ04416D

ether (5/1, v/v) as the eluent to give **MFNI**. Yield: 0.84g (42%). ^{1}H NMR (600 MHz, d6-DMSO) δ 10.17 (s, 1H), 8.57 (t, *J* = 7.8 Hz, 2H), 8.22 (d, *J* = 8.5 Hz, 1H), 8.14 (d, J = 8.1 Hz, 2H), 7.88 (t, J = 7.6 Hz, 2H), 7.81 (d, J = 8.1 Hz, 2H), 4.15 (t, J = 7.2 Hz, 2H), 3.43 (s, 4H), 2.40 (t, J = 6.8 Hz, 2H), 2.32 (s, 4H), 1.84 (dd, *J* = 14.2, 7.0 Hz, 2H). ^{13}C NMR (151 MHz, d6-DMSO) δ 195.08, 165.57, 165.35, 146.68, 146.19, 137.98, 133.88, 132.95, 132.80, 132.34, 131.92, 131.11, 130.27, 130.02, 129.94, 124.76, 124.19, 68.18, 58.03, 55.27, 40.50, 26.07. FTMS: m/z calcd for $C_{26}H_{24}N_2O_4$ ([M+H]$^+$): 429.1809; found 429.1807.

2.2.3. Synthesis of N-(morpholinopropyl)- 4-(4'-(2-picolinoylhydrazono)methyl) phenyl-1,8-naphthalimide ***CuNI***

N-(morpholinopropyl)- 4-formylphenyl-1,8-naphthalimide compound **MFNI** (0.107 g, 0.25 mmol) and 2-picolinyl hydrazide (0.038 g, 0.275 mmol) were stirred in ethanol (20 mL) containing 2–3 drops of acetic acid. The reaction was refluxed for 4 hours before cooling to room temperature. The solid product was filtered and recrystallized with ethanol for three times. Yield: 84%. ^{1}H NMR (600 MHz, DMSO) δ 12.28 (s, 1H), 8.80 (s, 1H), 8.75 (d, J = 4.2 Hz, 1H), 8.61 – 8.56 (m, 2H), 8.32 (d, J = 8.6 Hz, 1H), 8.17 (d, J = 7.7 Hz, 1H), 8.09 (t, J = 8.5 Hz, 1H), 7.96 (d, J = 8.2 Hz, 2H), 7.89 (m,2H), 7.70 (d, J = 8.1 Hz, 3H), 4.17 (d, J = 7.3 Hz, 2H), 3.43 (s, 4H), 2.41 (d, J = 6.8 Hz, 2H), 2.33 (s, 4H), 1.87 – 1.83 (m, 2H). ^{13}C NMR (151 MHz, d6-DMSO) δ 165.61, 165.39, 162.54, 151.57, 150.59, 150.55, 147.35, 141.75, 140.14, 136.62, 134.09, 132.87, 132.41, 131.21, 130.11, 129.74, 129.57, 129.15, 124.80, 124.72, 123.75, 68.14, 58.01, 55.04, 40.46, 26.04. FTMS: m/z calcd for $C_{32}H_{29}N_5O_4$ ([M+H]$^+$): 548.2292; found 548.2307.

2.3. *Spectroscopic measurements*

All spectral characterizations were carried out within a 10 mm quartz cell. The stock solution for **CuNI** (1 mM) was dissolved in HPLC grade DMSO at room temperature. Solutions of metal ions (1 mM) were prepared with nitrate or chloride salts in water. For a typical detection, 50 μL of **CuNI** stock solution (1 mM) was transferred to 5 mL flask and diluted to volume with water by 10 mM HOAc-NaOAc buffer (pH 5.0) to give the sample solution (10 μM). All the tests were carried out at room temperature.

The fluorescence quantum yields were obtained by HORIBA FluoroMax-4P (HORIBA Jobin Yvon). The compound **CuNI** solutions in the presence and the absence of Cu^{2+} were detected with the concentration of 10.0 μM (λex =370 nm, λem= 440 nm), respectively.

2.4. *Cytotoxicity test and cell culture*

The MTT (5-dimethylthiazol-2-yl-2,5-diphenyltetrazolium bromide) method was used to determine the toxicity of **CuNI** in HepG2 cells. HepG2 cells were passed and plated until they were 70% confluent in 96-well plates about 24 hours before treatment. Before the **CuNI** treatment, the DMEM (Dulbecco's Modified Eagle Medium) containing 10% FBS (Fetal Calf Serum) was removed, replaced with fresh DMEM, and an aliquot of **CuNI** stock solution (1 mM DMSO) was added to obtain the final concentration (0, 5, 10, 20 and 30 μM). The treated cells were incubated at 37°C and 5% CO_2 for 24 hours. Subsequently, the cells were treated with 5 mg/mL MTT (40 μL/well) and incubated for another 4 hours (37 °C, 5% CO_2). Use a microplate reader to measure the absorbance at 490 nm. Each individual cytotoxicity experiment was repeated three times.

HepG2 cells were incubated with **CuNI** (10 μM) and Lyso Tracker Red (500 nM) at 37 °C for 30 minutes. Washed with PBS for three times, and then the cells in the culture dish were collected for imaging of red channel and blue channel under confocal microscope. After incubating HepG2 cells with **CuNI** (10 μM) and Lyso Tracker Red (500 nM) for 30 minutes, they were washed three times with PBS, then Cu^{2+} (5 equiv.) was added, and the cells were incubated in a petri dish for 40 minutes. Finally, the red channel and blue were collected fluorescence image of the channel.

3. Results and discussion

3.1. Synthesis of CuNI

The synthesis of compound **CuNI** is depicted in (Scheme S1). And the compound **CuNI** was easily synthesized by the condensation reaction between **MFNI** and 2-picolinyl hydrazidein ethanol solvent. The structures of the intermediate and the final product were characterized by ^{1}H-NMR, ^{13}C-NMR and mass spectrometey（Fig. S1- Fig. S9）. The spectral data is consistent with the chemical structure of the compounds.

View Article Online
DOI: 10.1039/D0NJ04416D

ARTICLE

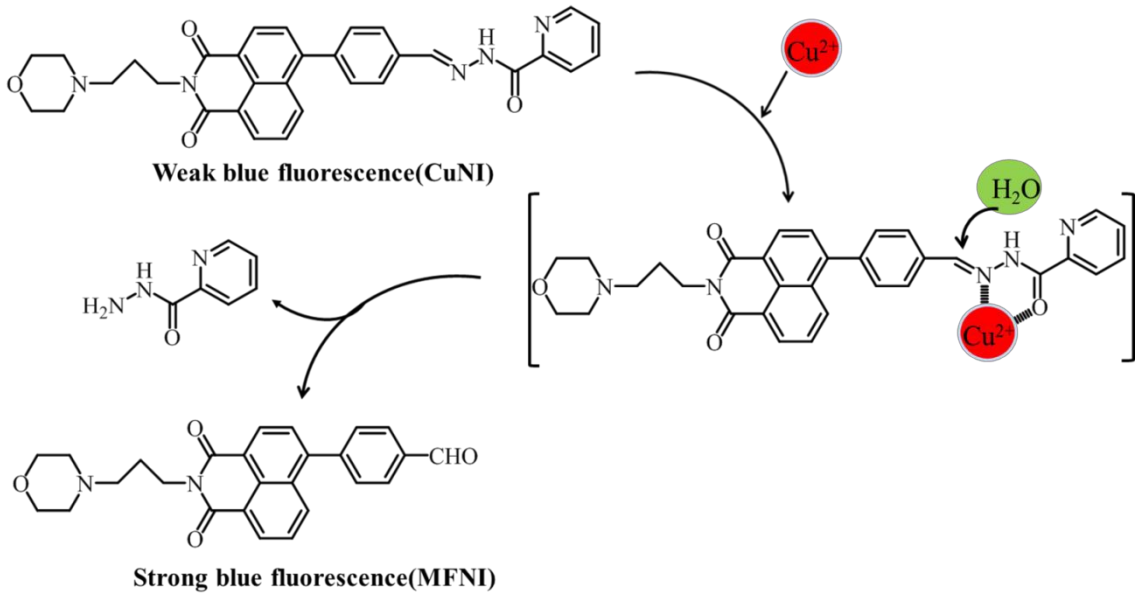

Scheme 1. Proposed mechanism of **CuNI** to Cu^{2+}

3.2. Fluorescence response of the probe CuNI to Cu^{2+}

In order to study the sensing ability of the probe **CuNI**, the emission behavior was monitored in the presence of various metal ions, including Cu^{2+}, Ca^{2+}, Al^{3+}, Cd^{2+}, Cr^{3+},Co^{2+}, Hg^{2+}, Fe^{3+}, Fe^{2+}, Na^{+}, K^{+}, Mg^{2+}, Ni^{2+}, Ba^{2+}, Pb^{2+}, Zn^{2+}, Hcy, Cys , GSH and ClO^{-} in HOAc-NaOAc buffer solution (Fig. 1). However, the addition of the other metal ions and small biological molecules have hardly changed the fluorescent signal. At the same time, it was shown that **CuNI** (10uM) under UV lamp only has obvious fluorescence enhancement when Cu^{2+} (5 equiv.) was added. (Fig. 2), which is consistent with the measured fluorescence spectrum phenomenon.The pure **CuNI** (10 μM) in HOAc-NaOAc buffer solution (pH 5.0) emitted weak fluorescence at 440nm with fluorescence quantum yield of 2.66% upon excited at 360nm. When Cu^{2+} (5 equiv.) was added into **CuNI** (10 μM) solution, the fluorescence emission intensity was increased significantly and the fluorescence quantum yield was increased from 2.66% to 39.31%. It is shown that **CuNI** has a significant fluorescence "turn-on" response to Cu^{2+}.

View Article Online
DOI: 10.1039/D0NJ04416D

ARTICLE

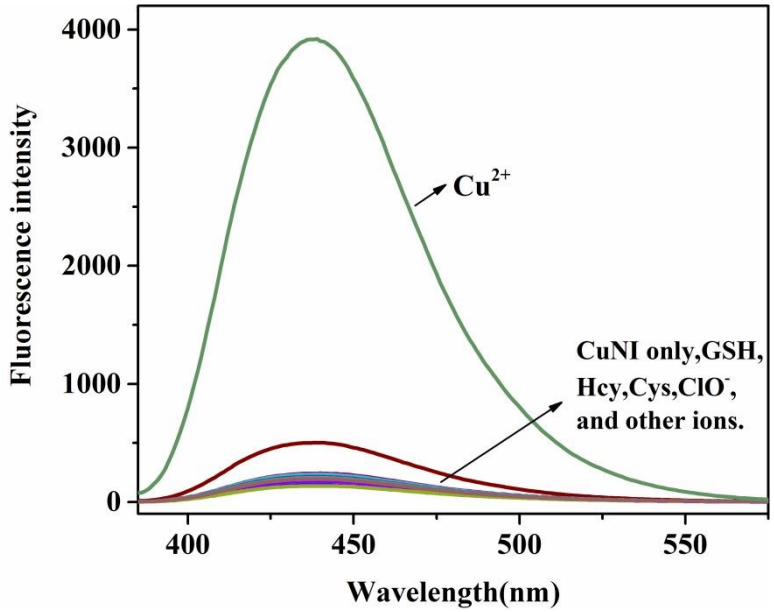

Fig. 1. Fluorescence spectra of **CuNI** (10 mM) to various metal ions, amino acids and ROS(ClO^-) (5 equiv.) at 25°C in HOAc-NaOAc buffer solution (10 mM, pH 5.0, with 1% DMSO) .

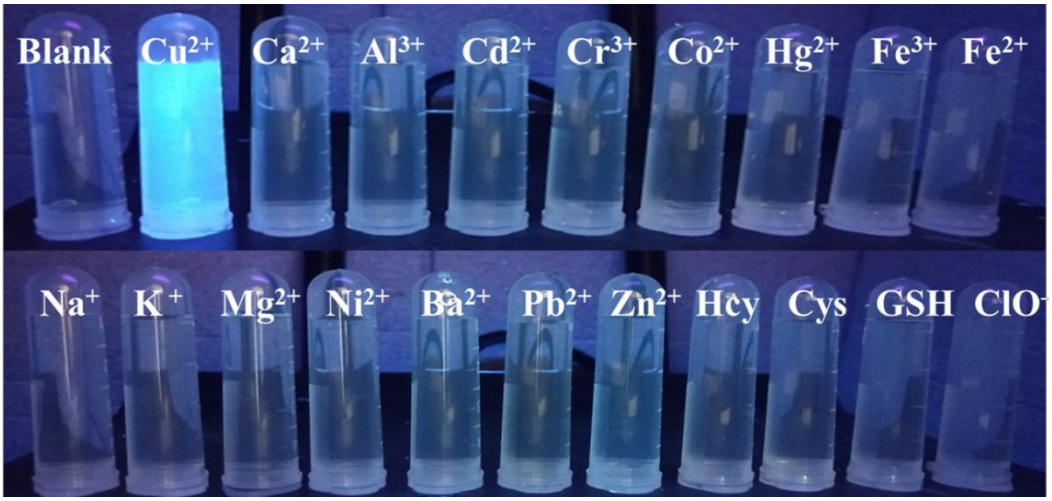

Fig. 2. Photograph of **CuNI** (10 mM) to various metal ions, amino acids and ROS (ClO^-) (5 equiv.) under UV lamp (λex 365 nm).

The selectivity of probe is an important parameter to evaluate the performance of probe. Therefore, competitive experiments were carried out on **CuNI** to test the fluorescence response of Cu^{2+} in the presence of other potential metal ions, amino acids and active oxygen ions. The fluorescence spectra show that the fluorescence intensity was still enhanced when the various distractors was added together with Cu^{2+}, and it was hardly interfered by other ions (Fig. 3). It is concluded that **CuNI** probe can be used to detect Cu^{2+} with high selectivity.

View Article Online
DOI: 10.1039/D0NJ04416D

ARTICLE

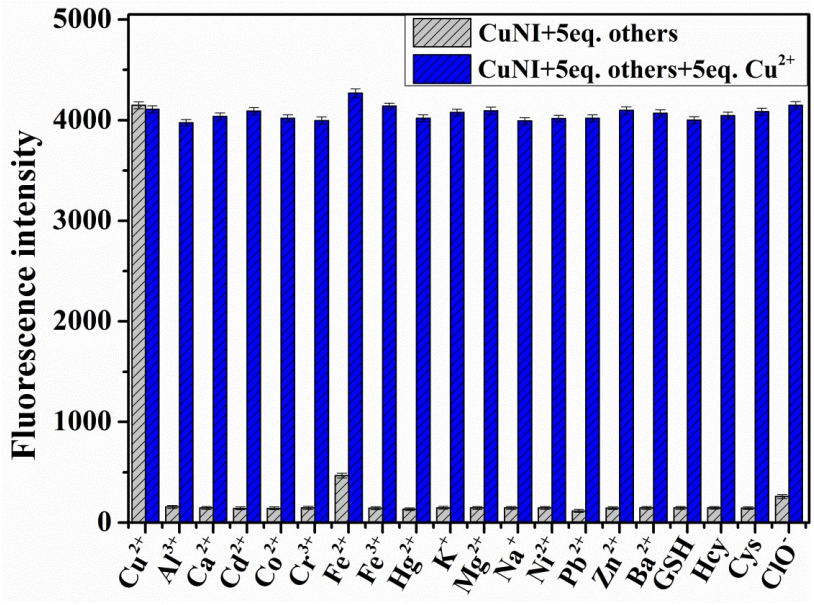

Fig. 3. The fluorescence intensity of **CuNI** (10 mmol) to others (Cu^{2+}, Al^{3+}, Ca^{2+}, Cd^{2+}, Co^{2+}, Cr^{3+}, Fe^{2+}, Fe^{3+}, Hg^{2+}, K^{+}, Mg^{2+}, Na^{+}, Ni^{2+}, Pb^{2+}, Zn^{2+}, Ba^{2+} ,Cys, Hcy, GSH, ClO^{-}) in HOAc-NaOAc buffer solution (10 mM, pH 5.0, 1% DMSO) at 25°C (λex =370 nm). The gray bar indicates the emission of **CuNI** in the presence of various metal ions, amino acids, and ROS(ClO^{-}) (5 equiv.). The blue bar represents the emission that occurs when various metal ions, amino acids, and ROS (ClO^{-}) (5 equiv.) and Cu^{2+} (5 equiv.) are added to the solution at the same time

The sensing characteristics of metal ions are usually demonstrated by fluorescence titration. Therefore, the fluorescence titration of Cu^{2+} with probe **CuNI** was carried out in HOAc-NaOAc buffer solution (pH 5.0). As shown in (Fig. 4), with the increase of Cu^{2+} concentration, the fluorescence intensity also increase gradually. The data shows that the amount of Cu^{2+} added was from 0 to 1.0 equivalent, and the linear relationship between the fluorescence emission intensity and Cu^{2+} was good.The fluorescence detection limit (LOD) of **CuNI** for Cu^{2+} can be calculated from the standard curve of concentration titration experiment. A good linear relationship between I_{400nm} and $[Cu^{2+}]$ in the range 2-10 uM（R^2=0.9940）(Fig. S10). The line equation was F_{440nm}=1271.5111+2.6510E8 $[Cu^{2+}]$. From the formula LOD =3σ/k, where k is the slope of the correction curve and σ is the standard deviation of the blank measurement [38]. The LOD is as low as 19.4 nM. This value was much lower than the detection line of other fluorescent probes used to detect the level of Cu^{2+} in the lysosome[39]. The results show that the probe **CuNI** can detect Cu^{2+} sensitively.

NJC A novel "turn-on" fluorescent probe based on naphthalimide for the tracking of lysosomal Cu2+ in living cells

ARTICLE

View Article Online
DOI: 10.1039/D0NJ04416D

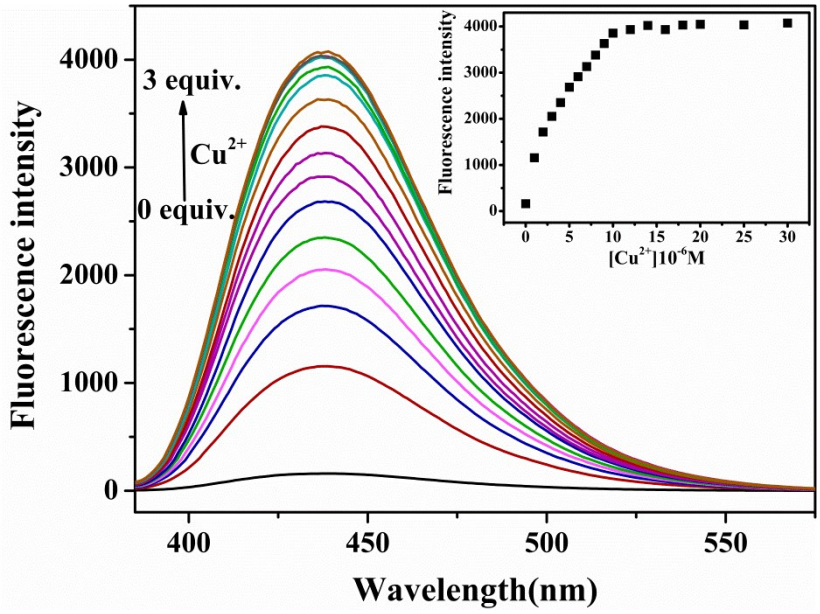

Fig. 4. Fluorescence spectra (λex =370 nm) of **CuNI** (10 mM) with increasing Cu^{2+} content in HOAc-NaOAc buffer solution (10 mM, pH 5.0, 1% DMSO) at 25°C. Inset: Relationship between fluorescence intensity ($I_{440\,nm}$) and Cu^{2+} concentration.

In addition, the suitable pH range for Cu^{2+} sensing was also investigated, we explored the fluorescence emission intensity (F_{440nm}) at different pH (pH 3.0-10.0) (Fig S11). In the absence of Cu^{2+}, the fluorescence intensity of probe **CuNI** (10 μM) maintains weak fluorescence emission intensity in the pH range from 3.00 to 10.00. When Cu^{2+}（5equiv.） exists in the probe **CuNI** solution, the fluorescence emission intensity changes significantly. When pH⩽7, the fluorescence emission intensity in the presence of Cu^{2+} maintains strong emission. When pH>7, as the pH gradually increases, the fluorescence emission intensity gradually decreases. Because the lysosomal environment is pH 5, it provides suitable pH conditions for the probe and Cu^{2+}. This indicates that the probe **CuNI** may trace Cu^{2+} in the lysosome

Subsequently, the fluorescence emission spectra of **CuNI** (10 μM) and Cu^{2+} (5 equiv.) over time were tested in an HOAc-NaOAc buffer solution at room temperature. With the increase of time, the fluorescence emission peak at 440 nm gradually increased and reached equilibrium after about 40 min (Fig. S12). This indicates that **CuNI** can react with Cu^{2+} completely after 40 min.

3.3. Mechanism of the probe CuNI in sensing Cu^{2+}

Considering the ease of the Schiff base hydrolysis in aqueous medium and good affinity of the hydrazide group for Cu^{2+}, we deduce that the Cu^{2+} firstly coordinates with the oxygen and nitrogen atoms of the probe **CuNI**, hydrolyzed to afford the aldehyde (compound **MFNI**) and then lead to the "turn-on" fluorescence, which is illustrated in (Scheme 1). This can be testified by that the fluorescence spectrum of the **CuNI** solution added with Cu^{2+} is very similar to those of **MFNI** (Fig. 5). The sensing mechanism can be further reasonably explained by ^1H NMR titration (Fig. 6). The Fig. 6 shows the signal peak range of the benzene ring region and the aldehyde proton peak. With the addition of various equivalents of Cu^{2+} into the solution (DMSO-d6) of **CuNI**, the peak at 10.17 ppm assigned to the aldehyde (**MFNI**) proton appeared gradually. The complete titration is shown in Fig. S13 . At the same time, the reaction between **CuNI** and Cu^{2+} was confirmed by FTMS (ESI). With the presence of Cu^{2+}, the peak of **CuNI** (m/z 548.23 $[M+H]^+$) disappeared, while a new peak emerged at m/z 429.18 $[M+H]^+$ (Fig. S14), which represented the formation of the aldehyde (compound **MFNI**).

View Article Online
DOI: 10.1039/D0NJ04416D

ARTICLE

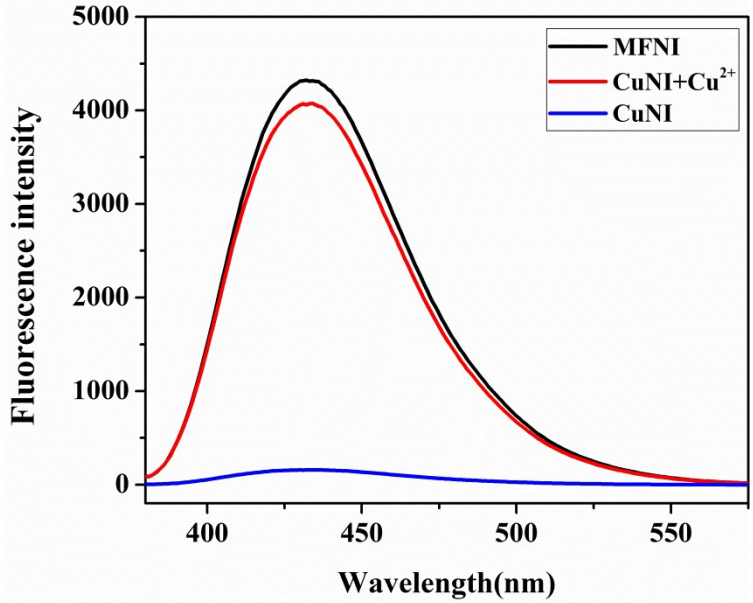

Fig. 5. Fluorescence spectra (λex =370 nm) of **MFNI**, **CuNI** and **CuNI** + Cu^{2+} (5 equiv.) in HOAc-NaOAc buffer solution (10 mM, pH 5.0, with 1% DMSO)

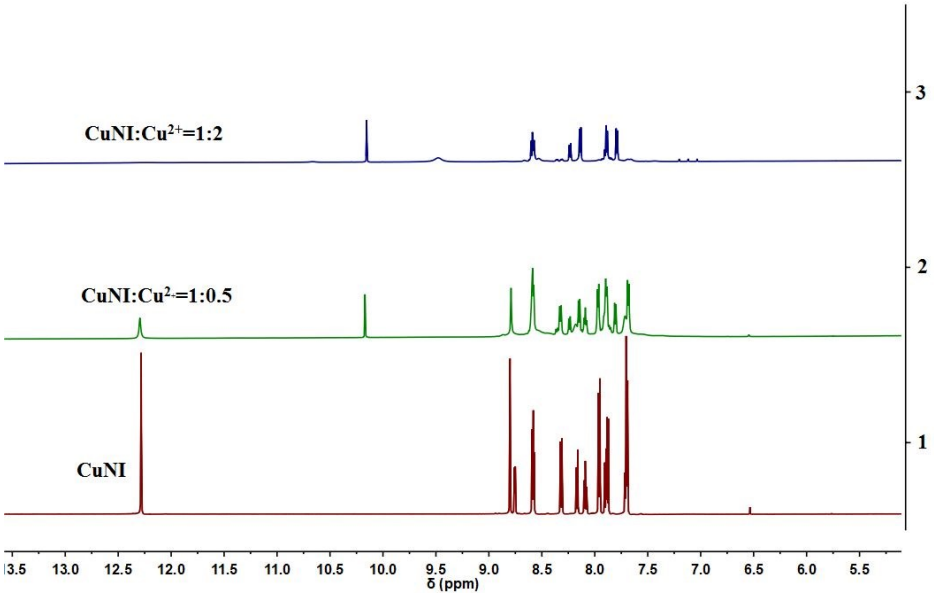

Fig. 6. ^{1}H NMR spectra of (1) **CuNI** in DMSO-d6, (2) **CuNI** in DMSO-d6 + Cu^{2+} (0.5 equiv.) in D_2O, (3) **CuNI** in DMSO-d6 + Cu^{2+} (2 equiv.) in D_2O.

We investigated the influence of solvent to the fluorescence of probe further. The recognition of probe **CuNI** to Cu^{2+} distinctly showed the aggregation induced emission feature. As presented in (Fig. 7a), with addition of Cu^{2+} into the probe **CuNI**, extremely weak fluorescence signals at 438 nm were observed when probe dissolved in a good solvent, such as <60% water fraction. Nevertheless, when a large amount of HOAc-NaOAc buffer was

View Article Online
DOI: 10.1039/D0NJ04416D

added into the DMSO solution (fw> 80%), the fluorescence intensity increased dramatically under identical measurement conditions and the blue emission became visible. As fw increased to 99%, the emission intensity of the system is approximately 100-fold higher than that in fw 10% HOAc-NaOAc buffer/DMSO solution (Fig. 7b). This result shows that the recognition of probe **CuNI** to Cu^{2+} possesses typical AIE characteristics.

To further confirmed the AIE feature, DLS (dynamic light scattering) and SEM (scanning electron microscope) were performed for the probe **CuNI** (10 μM) with the addition of Cu^{2+} in DMSO/HOAc-ONaAc buffer (1:99, v/v). The DLS measurement shows the presence of nanoparticles with average sizes of ca. 115.7 nm (Fig. 7c). SEM results show that the particle size is about 150 nm (Fig. 7d). As shown in Fig. S15a, TEM results show that the average size is about 100nm. Fig. S15b magnifies individual particles, and the results show that the particles are aggregates of organic matters. Both SEM, DLS and TEM show the conformation of the nanoaggregates. Combined with the mechanism of the probe **CuNI** in sensing Cu^{2+}, we could deduce that the hydrolysis of probe **CuNI** was happened with the addition of Cu^{2+}, and the aldehyde **MFNI** generated with the hydrolysis reaction can aggregate-induced emit the bright blue fluorescence in aqueous solution.

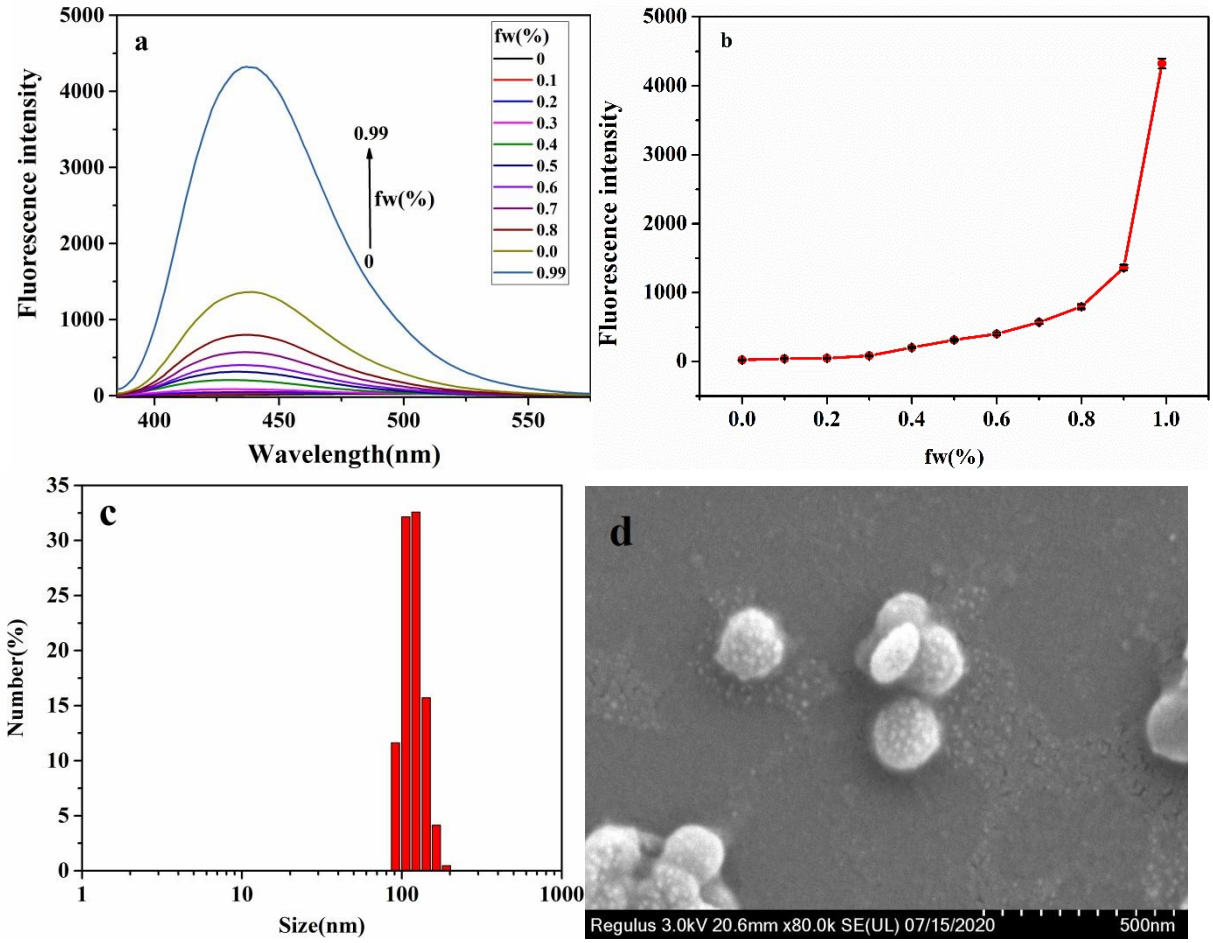

Fig. 7. (a) Fluorescence spectrum of **CuNI** (10 μM) in DMSO/ HOAc-NaOAc buffer solution (10 mM, pH 5.0) with different water fractions added with Cu^{2+} (5equiv.)(λex=370nm). (b) The fluorescence intensity changes of **CuNI** (10 μM) in DMSO/ HOAc-NaOAc buffer solution (10 mM, pH 5.0) with different water fractions added with Cu^{2+} (5equiv.) (λex=370nm). (c) Particle size distributions of **CuNI** (10 μM) added with Cu^{2+} (5 equiv.) in HOAc-NaOAc buffer solution (10 mM, pH 5.0, with 1% DMSO). (d) SEM of **CuNI** (10 μM) added with Cu^{2+} (5 equiv.) in HOAc-NaOAc buffer solution (10 mM, pH 5.0, with 1% DMSO).

3.4 Cytotoxicity and cell imaging

To further value the practical utilization of **CuNI**, we tested the applicability of **CuNI** for sensing Cu^{2+} in living cells and the HepG2 cells were used as the model cells. As a probe used in living cells, biocompatibility is usually the first property to be examined. The cytotoxic effect of **CuNI** was determined via an MTT (5-dimethylthiazol- 2-yl-2,5- diphenyltetrazolium bromide) assay before it used for cell imaging. As shown in (Fig. S16), the cell

View Article Online
DOI: 10.1039/D0NJ04416D

survival rates are above 80% when incubated with 30 μM of **CuNI** after 24 h. The results showed that the toxicity of **CuNI** to cells could be ignored when the concentration of **CuNI** reached 30 μM and incubated for a long time, which was obviously beneficial to cell imaging.

Moreover, we evaluated the applicability of **CuNI** in imaging lysosomal Cu^{2+} in living cells by a confocal fluorescence microscope. HepG2 cells were incubated with **CuNI** (10 μM) and Lyso Tracker Red (500 nM) at 37 °C for 30 min. As shown in (Fig. 8a), the blue channel fluorescence emission of HepG2 cells treated with **CuNI** for 30 min is very weak and can be ignored. As shown in (Fig. 8b), a clear lysosomal position with strong red fluorescence was observed, which was attributed to Lyso Tracker Red. After incubation of HepG2 cells with **CuNI** (10 μm) and Lyso Tracker Red (500 nM) at 37 °C for 30 min, the cells were incubated with Cu^{2+} (50 μM) for 40 min. As shown in(Fig. 8e, Fig. 8f), the blue channel obtained strong fluorescence, which was similar to lysosomal spectrum, and the linear regions of interest (ROIs) (**CuNI** and Lyso Tracker Red co-staining).The change of intensity distribution is synchronous, and the fluorescence signal of probe overlaps well with that of Lyso Tracker Red(Fig. 8h). In addition, Pearson's co-localization coefficients were used to quantify the co-localization. The correlation diagram describes the distribution between the intensity of the two channels. As shown in (Fig. 8i), it shows a good co-localization coefficient (R = 0.9112). It can be seen that the probe **CuNI** targets the position of the lysosome of HepG2 cells and can detect Cu^{2+} in the lysosome.

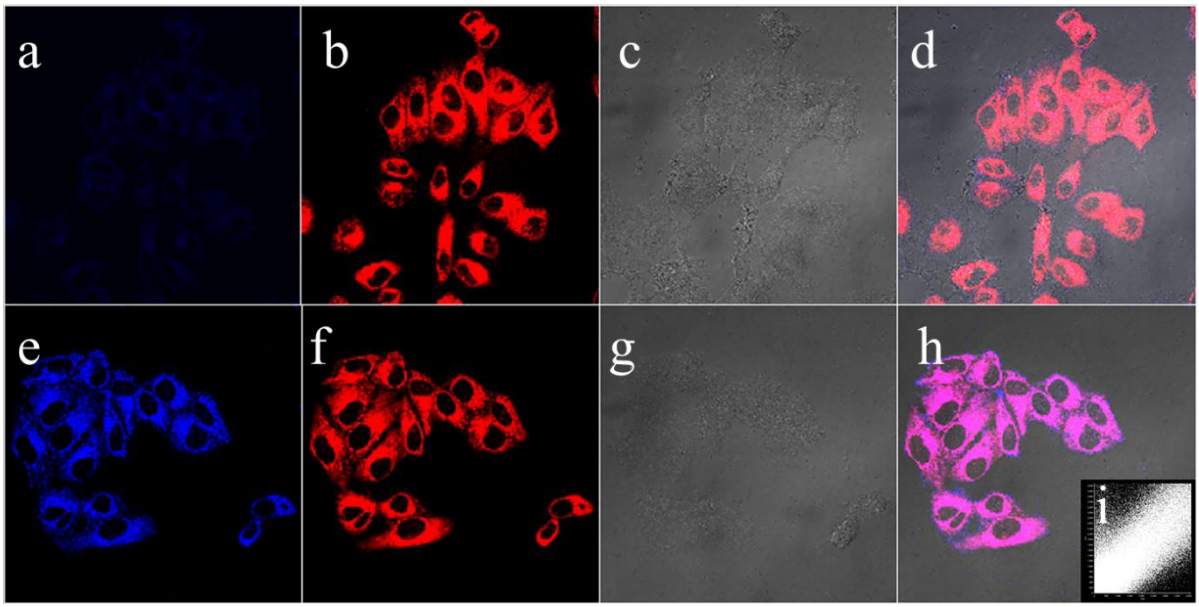

Fig. 8. Confocal images of HepG2 cells. (a-d) **CuNI** (10 μM) and Lyso Tracker Red (500 nM) were incubated together at 37 °C for 30 minutes, (e-h) **CuNI**(10 μM) and Lyso Tracker Red (500 nM) were incubated together at 37 °C for 30 minutes, and then incubated with Cu^{2+} (50 μM) for 40 minutes, (a, e) image of blue channel, (b, f) image of red channel, (c, g) image of bright field, (d) overlay image of (a ,b and c). (h) overlay image of (e, f and g). (i) Linear relationship between blue channel and red channel

4. Conclusion

In short, this article describes a new type of fluorescent probe **CuNI** for the detection of lysosomal is visible to the naked eye under UV lamp. The investigation of the recognized mechanism is demonstrated that Cu^{2+} promoted interact with Cu^{2+} through hydrolysis of **CuNI** under acid condition and the hydrolysate **MFNI** has an obvious AIE effect which emit the bright blue fluorescence in aqueous solution. **CuNI** also have good biocompatibility and can detect Cu^{2+} in the lysosome of living HepG2 cells.

Conflicts of interest

There are no conflicts to declare.

Acknowledgements

This research is financially supported by the National Natural Science Foundation of China (No. 21404001), the Anhui Province

University Natural Science Research Project (No. KJ2017A008) and the Anhui Provincial Natural Science Foundation (No.1808085ME55) and National Training Programs of Innovation and Entrepreneurship for Undergraduates (No. 201910357045).

Notes and references

1. V. Desai and S. G. Kaler, *The American Journal of Clinical Nutrition*, 2008, **88**, 855-858.
2. Y. Zhang, M. Li, Q. Yao and C. Chen, *Medical Science Monitor*, 2009, **15**, RA1-RA5.
3. M. Vetchý, *Ceska a Slovenska farmacie : casopis Ceske farmaceuticke spolecnosti a Slovenske farmaceuticke spolecnosti*, 2018, **67**, 143-153.
4. S. Feng, S. Hou, Y. Cui, Y. Tong and H. Yang, *Journal Of Industrial Microbiology & Biotechnology*, 2020, **47**, 21-33.
5. L. M. Gaetke, H. S. Chowjohnson and C. K. Chow, *Archives of Toxicology*, 2014, **88**, 1929-1938.
6. R. I. Spain, T. P. Leist and E. A. De Sousa, *Nat Clin Pract Neurol*, 2009, **5**, 106-111.
7. E. L. Jensen, A. M. Gonzalez-Ibanez, P. Mendoza, L. M. Ruiz, C. A. Riedel, F. Simon, J. J. Schuringa and A. A. Elorza, *Metallomics*, 2019, **11**, 282-290.
8. H. Kodama, C. Fujisawa and W. Bhadhprasit, *Current Drug Metabolism*, 2012, **13**, 237-250.
9. E. S. Ford, *American Journal of Epidemiology*, 2000, **151**, 1182-1188.
10. E. Gaggelli, H. Kozlowski, D. Valensin and G. Valensin, *Chemical Reviews*, 2006, **106**, 1995-2044.
11. M. C. Miotto, E. E. Rodriguez, A. A. Valiente-Gabioud, V. Torres-Monserrat, A. Binolfi, L. Quintanar, M. Zweckstetter, C. Griesinger and C. O. Fernandez, *Inorganic Chemistry*, 2014, **53**, 4350-4358.
12. P. V. E. V. Den Berghe, D. E. Folmer, H. E. M. Malingre, E. A. C. M. Van Beurden, A. E. M. Klomp, B. V. De Sluis, M. Merkx, R. Berger and L. W. J. Klomp, *Biochemical Journal*, 2007, **407**, 49-59.
13. B. L. Logeman, L. K. Wood, J. Lee and D. J. Thiele, *Journal Of Biological Chemistry*, 2017, **292**, 11531-11546.
14. A. P. S. Gonzáles, M. A. Firmino, C. S. Nomura, F. R. P. Rocha, P. V. Oliveira and I. Gaubeur, *Analytica Chimica Acta*, 2009, **636**, 198-204.
15. C. F. Harrington, S. A. Merson and T. M. D. Silva, *Analytica Chimica Acta*, 2004, **505**, 247-254.
16. D. Shan, C. Mousty and S. Cosnier, *Analytical Chemistry*, 2004, **76**, 178-183.
17. Y. Fu, X.-X. Pang, Z.-Q. Wang, Q. Chai and F. Ye, *Spectrochimica Acta Part A: Molecular and Biomolecular Spectroscopy*, 2019, **208**, 198-205.
18. Z. E. Chen, X. F. Zang, M. Yang and H. Zhang, *Spectrochimica Acta Part a-Molecular and Biomolecular Spectroscopy*, 2020, **234**.
19. Y. Li, H. Lan, X. Yan, X. Shi, X. Liu and S. Xiao, *Spectrochimica Acta Part A: Molecular and Biomolecular Spectroscopy*, 2020, **227**, 117565.
20. Y. H. Li, Y. R. Zhao, W. H. Chan, Y. J. Wang, Q. H. You, C. H. Liu, J. Zheng, J. S. Li, S. Yang and R. H. Yang, *Analytical Chemistry*, 2015, **87**, 584-591.
21. K. S. Mani, R. Rajamanikandan, B. Murugesapandian, R. Shankar, G. Sivaraman, M. Ilanchelian and S. P. Rajendran, *Spectrochimica Acta Part A: Molecular and Biomolecular Spectroscopy*, 2019, **214**, 170-176.
22. Z. Gu, H. Cheng, X. Shen, T. He, K. Jiang, H. Qiu, Q. Zhang and S. Yin, *Spectrochimica Acta Part A: Molecular and Biomolecular Spectroscopy*, 2018, **203**, 315-323.
23. J. Zhang, M. Zhu, D. Y. Jiang, H. Zhang, L. Y. Li, G. N. Zhang, Y. C. Wang, C. Feng and H. Zhao, *New Journal Of Chemistry*, 2019, **43**, 10176-10182.
24. S. Swami, D. Behera, A. Agarwala, V. P. Verma and R. Shrivastava, *New Journal Of Chemistry*, 2018, **42**, 10317-10326.
25. A. S. Ren, D. J. Zhu, W. Xie, X. C. He, Z. H. Duan, Y. H. Luo, X. Zhong, M. B. Song and X. W. Yan, *Inorganica Chimica Acta*, 2018, **476**, 136-141.
26. M. Li, H. Chen, X. Liu, N. Zhang, Q. Sun and K. Zheng, *Inorganica Chimica Acta*, 2020, **511,**119825.
27. K. Huang, D. Han, X. Li, M. Peng, X. Zeng, L. Jing and D. Qin, Dyes and Pigments, 2019, 171, 107701.
28. Y. Yaling and Y. I. He, *Analytical Sciences*, 2019, **35**, 159-163.
29. X. Li, Y. Guo, T. Xu, M. Fang, Q. Xu, F. Zhang, Z. Wu, C. Li and W. Zhu, *Journal Of the Chinese Chemical Society*, 2020, **67**, 1070-1077.
30. N. Khac Hong, Y. Hao, K. Zeng, X. Wei, S. Yuan, F. Li, S. Fan, M. Xu and Y.-N. Liu, *Journal Of Photochemistry And Photobiology a-Chemistry*, 2018, **358**, 201-206.
31. K. Wechakorn, S. Prabpai, K. Suksen, P. Kanjanasirirat, Y. Pewkliang, S. Borwornpinyo and P. Kongsaeree, *Luminescence*, 2018, **33**, 64-70.
32. D. Zhu, A. Ren, X. He, Y. Luo, Z. Duan, X. Yan, Y. Xiong and X. Zhong, *Sensors and Actuators B: Chemical*, 2017, **252**, 134-141.
33. P. Gopikrishna, N. Meher and P. K. Iyer, *Acs Applied Materials & Interfaces*, 2017, **10**, 12081-12111.
34. R. T. K. Kwok, C. W. T. Leung, J. W. Y. Lam and B. Z. Tang, *Chemical Society Reviews*, 2015, **44**, 4228-4238.
35. J. Harathi and K. Thenmozhi, *Materials Chemistry Frontiers*, 2020, **4**, 1471-1482.
36. G.-J. Mao, Z.-Z. Liang, G.-Q. Gao, Y.-Y. Wang, X.-Y. Guo, L. Su, H. Zhang, Q.-J. Ma and G. Zhang, *Analytica Chimica Acta*, 2019, **1092**, 117-125.
37. W. N. Wu, H. Wu, R. B. Zhong, Y. Wang, Z. H. Xu, X. L. Zhao, Z. Q. Xu and Y. C. Fan, *Spectrochimica Acta Part a-Molecular and Biomolecular Spectroscopy*, 2019, **212**, 121-127.
38. S. W. Cho, A. S. Rao, S. Bhunia, Y. J. Reo, S. Singha and K. H. Ahn, *Sensors And Actuators B-Chemical*, 2019, **279**, 204-212.
39. Y. Fu, X. X. Pang, Z. Q. Wang, Q. Chai and F. Ye, Spectrochimica Acta Part a-Molecular And Biomolecular Spectroscopy, 2019, 208, 198-205.

View Article Online
DOI: 10.1039/D0NJ04416D

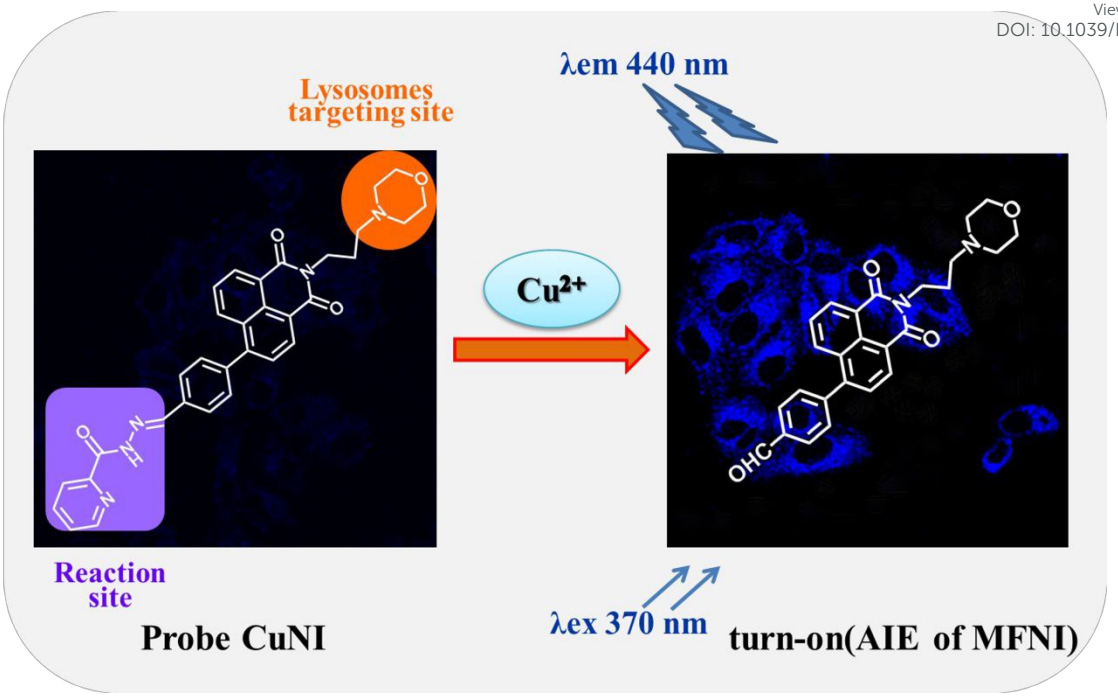

The probe **CuNI** was synthesized based on the naphthimide fluorophore. **CuNI** emits weak blue fluorescence in aqueous solution. **CuNI** breaks the C=N bond through hydrolysis to obtain **MFNI**, which emits strong blue fluorescence when Cu^{2+} is present. This is mainly because **MFNI** has obvious AIE phenomenon. The detection limit of **CuNI** for Cu^{2+} is 19.40 nM. In HepG2 cells, the presence of Cu^{2+} still shows obvious fluorescence enhancement. This shows that **CuNI** can not only have good selectivity to Cu^{2+} in aqueous solution, but also has a good targeting function for Cu^{2+} in lysosomes.